

MID-INFRARED FEATURES OF KAOLINITE-DICKITE

JAVIER CUADROS*, RAQUEL VEGA, AND ALEJANDRO TOSCANO

Department of Earth Sciences, Natural History Museum, Cromwell Road, London SW7 5BD, UK

Abstract—Transformation of kaolinite to dickite is a common diagenetic reaction. The present report is part of a wider study to investigate the pathways of this polytype change. Fourier-transform infrared spectroscopy (FTIR) was used to attempt quantification of the relative proportions of kaolinite and dickite, validated by X-ray diffraction (XRD) results, in order to link mineral and structural features during the mineralogical changes. A group of kaolinite and dickite samples was investigated: 13 samples from the Frøy and Rind oil fields (North Sea), three kaolinite specimens with different crystal order and particle size (KGa-2, kaolinite API 17, Keokuk kaolinite), and two dickite-rich samples (Natural History Museum collection). Six FTIR spectral features were analyzed: (1) intensity ratio of the minima at 3675 and 3635 cm^{-1} ; (2) position of the band at $\sim 1115 \text{ cm}^{-1}$; (3) difference between the frequency of the bands at ~ 1030 and $\sim 1000 \text{ cm}^{-1}$; (4) intensity ratio of the bands generating shoulders at ~ 922 and $\sim 900 \text{ cm}^{-1}$; (5) position of the band at $\sim 370 \text{ cm}^{-1}$; and (6) intensity of the band at $\sim 268 \text{ cm}^{-1}$. Correlation of the features above with polytype relative proportions derived from XRD showed non-linear behavior, with maximum curvature at the dickite end, which precludes kaolinite-dickite quantification. Increasing kaolin particle size is known to cause decreased intensity of the FTIR spectra. A model was developed to test whether this effect is consistent with the non-linear progression of the IR features. The relative intensity of kaolinite and dickite IR features were calculated in a series of kaolinite-to-dickite transformations, where the size of particles increases with dickite proportion, and where dickite-dominated particles reach a larger size than kaolinite-dominated particles. The results indicated that the differential particle size increase is possibly the cause of the lack of linearity between IR- and XRD-measured dickite proportions.

Key Words—Dickite, Infrared Spectroscopy, Kaolinite.

INTRODUCTION

Numerous authors have investigated the infrared (IR) and Raman characteristics of the several kaolin polytypes. The most recent studies, which benefit from previous work and in which other references can be found, are cited here. Much attention has been given to hydroxyl stretching vibrations, in experimental (*e.g.* Prost *et al.*, 1989; Frost 1997; Shoval *et al.*, 1999, 2002; Johnston *et al.*, 2008) and theoretical (*e.g.* Benco *et al.*, 2001) studies, given the clear differences between the signatures of the several kaolin polytypes. Studies have also focused on hydroxyl deformation (*e.g.* Frost, 1998) and lattice vibrations (*e.g.* Frost 1997). The studies listed above deal with band assignment and try to relate specific spectral characteristics with polytype structural features. Especially interesting were the low-temperature (up to 10 K) studies by Prost *et al.* (1989), Johnston *et al.* (2008), and Balan *et al.* (2010) because the low-temperature spectra are better resolved and facilitate band assignments. Those studies were able to identify diagnostic vibrations for each polytype. Balan *et al.* (2010) observed a kaolinite band in dickite produced by a kaolinite-like stacking defect. Dickite and nacrite bands in kaolinite samples were observed by Prost *et al.*

(1989) and Johnston *et al.* (2008). Whether dickite and nacrite were present in kaolinite crystals or as separate crystals could not be inferred from the IR study. However, evidence for their existence within kaolinite crystals was found by Johnston *et al.* (2008) in the fact that selected area electron diffraction patterns (SAED) of ordered kaolinite displayed streaking indicating interstratification of kaolinite, dickite, and nacrite polytypes. An IR microspectroscopic technique has been developed (Robin *et al.*, 2013) that is an important step toward discriminating between interstratified and segregated kaolin polytypes.

The different spectral shapes of kaolinite and dickite suggest that IR spectroscopy can be used to quantify the relative proportions of the two polytypes when they occur together. Certainly, semi-quantitative assessments are possible and relatively simple (*e.g.* Lanson *et al.*, 2002). A full quantification of the relative proportions of polytypes from a kaolinite-to-dickite transformation series was carried out by Cassagnabère (1998). However, accurate quantification of kaolinite and dickite with IR methods may not be possible due to interaction phenomena between the crystals and the IR radiation. For example, changes in the relative intensity of hydroxyl stretching bands of kaolinite related to crystal size and orientation of the OH vectors were found by Shoval *et al.* (1999, 2002). OH-stretching absorptivity in a variety of minerals, including kaolinite, dickite, and nacrite, was found by Balan *et al.* (2008) to depend on the frequency of the specific OH-stretching band. Brindley *et al.* (1986)

* E-mail address of corresponding author:

j.cuadros@nhm.ac.uk

DOI: 10.1346/CCMN.2015.0630201

found that samples with high crystal order had spectra of lower intensity than samples of low crystal order, and Johnston *et al.* (2008) reported wider bands and distorted features in highly crystalline samples. In the present study, a full IR-based quantification of kaolinite and dickite was attempted in samples from the North Sea as part of a wider investigation of kaolinite transformation to dickite (Cuadros *et al.*, 2014; unless stated otherwise, the word “transformation” does not imply a specific reaction mechanism). The goal was to compare FTIR spectroscopy and XRD results from the quantification of the relative proportions of kaolinite and dickite in order to establish links between the structural features of the two polytypes probed by these techniques.

MATERIALS AND METHODS

Samples

The samples analyzed are those investigated by Cuadros *et al.* (2014) and consist of three groups. The first group of samples is a series of kaolinite-dickite core specimens of diagenetic origin from the Frøy and Rind oil fields, Norwegian Continental Shelf, North Sea (ELK series) which were part of a collection in Poitiers, France (Cassagnabère, 1998). The samples consist of sandstones and shales. An error exists in the Cuadros *et al.* (2014) study, as the samples in that and the present study are unrelated to the ‘Broad Fourteens’ basin. For this reason some of the references in Cuadros *et al.* (2014) do not apply to the samples in the present study and previous references about them should be taken from the present article. The original wells from which the samples were recovered can be located with the identification provided (Table 1) using Cassagnabère (1998, table II-3 and figure II-9 therein) and the world wide web. The samples were made available by C. Fialips (Total, Pau, France) and D. Beaufort (HydrASA team, IC2MP Laboratory, UMR 7285 CNRS-Université de Poitiers, France), and were studied as received. They are the 5–10 μm size fraction of specimens from depths of 3036–4520 m. The original samples were dry-ground to <2 mm grain size, dispersed in water by ultrasonic treatment, separated by sedimentation, and hydrocarbons were removed by Soxhlet extraction using chloroform (Cassagnabère, 1998). Kaolinite was either of detrital origin or formed from K-feldspar and then transformed to dickite with burial. Maximum temperatures experienced by the sediments ranged from 100 to 110°C (Beaufort *et al.*, 1998) for samples from depths of 3000–3585 m (Cuadros *et al.*, 2014). Sample ELK91, however, was drilled from a depth of 4519 m, for which no maximum temperature is known to the authors. For further information, refer to Beaufort *et al.* (1998) and Cassagnabère (1998).

The second group of samples consisted of three kaolinites: (1) kaolinite KGa-2, from Warren County, Georgia, USA, is of supergene origin, a product of a

Table 1. % dickite from XRD in the kaolinite-dickite samples with corresponding standard deviation (2σ), and identification of the well from which the North Sea samples originated.

Sample	Well	% Dickite	St. dev.
KGa-2		0	
Kaol 17		0	
Keokuk		0	
ELK 76	25/5-1	42	16
ELK 33	25/2-14	67	15
ELK 9	25/5-2	91	2
ELK 22	25/2-5	92	5
ELK 43	25/2-6	72	8
ELK 5	25/2-6	83	5
ELK 67	25/2-13	86	8
ELK 84	25/2-13	89	2
ELK 11	25/2-13	90	5
ELK 63	25/5-A3	84	10
ELK 88	25/5-A3	90	2
ELK 53	25/2-15R2	94	7
ELK 91	25/5-A7	93	6
BM 1923		92	10
BM 1927		89	7

complex alteration history and has low crystal order. Its geological context was described by Moll (2001). The sample was obtained from the Source Clays Repository of The Clay Minerals Society. (2) Kaolinite API 17 (labeled here as Kaol 17) from Lewistown, Montana, USA, is one of the reference materials from the American Petroleum Institute Project 49. It originated through hydrothermal alteration of feldspar in a syenite porphyry. The geological description can be found in Kerr and Kulp (1949), where this specimen was originally described as dickite, although it was later demonstrated to be kaolinite (Lindberg and Smith, 1974). This kaolinite is of intermediate crystal order. (3) Keokuk kaolinite (labeled here as Keokuk) is a specimen of very high crystal order which originated from geodes in Keokuk, Iowa, USA. The processes that produced the Keokuk geodes were described by Hayes (1936) as far as they were understood. The accepted interpretation is that kaolinite precipitated in voids produced by carbonate dissolution, from fluids generated after silicate-mineral dissolution. No reference is made in this interpretation to hydrothermal activity. Kaolinite from some of the snow-white patches in one of the geodes was scratched off with a needle. The three kaolinites (KGa-2, Kaol 17, and Keokuk) were ground gently, by hand, with mortar and pestle. No other treatment was performed. The third group of samples consisted of two dickites from the collection in the Natural History Museum (London). (1) Dickite BM 1927, 60 (labeled here as BM 1927) is from a massive slate collected in Kolno, Nowa Ruda, Silesia, Poland. Zimmerle and Rösch (1990) indicate that the presence of dickite in this area is related to hydrothermal activity.

Some material from the slate was scratched off using a needle. (2) Dickite BM 1923, 393 (hereafter BM 1923) is from Red Mountain, San Juan County, Colorado, USA. No other information is available. The specimen consisted of sub-mm-sized crystals, of which an aliquot was collected. The dickites were ground as indicated above for the kaolinites. The previous scanning electron microscopy (SEM) and XRD study (Cuadros *et al.*, 2014) demonstrated that the grinding procedure preserved the original particle size of individual crystals and their coherent scattering domain sizes because after the same grinding treatment each sample had different values for the above variables.

Previous characterization

These samples were characterized thoroughly using XRD, thermal analysis, and SEM (Cuadros *et al.*, 2014). The relative proportion of kaolinite and dickite in the samples was quantified using XRD analysis (Table 1; see Cuadros *et al.*, 2014). Non-kaolin minerals were present in minor to trace proportions. Further XRD, thermal, and SEM analysis allowed detailed investigation of the crystal and morphological characteristics of the samples. The main information from Cuadros *et al.* (2014) of relevance to the IR study is: (1) the samples cover a range of increasing crystal order (and particle size) in this order: KGa-2, Kaol 17, Keokuk, and ELK samples with less dickite content, and finally ELK samples with more dickite content, and the BM samples;

(2) in samples containing kaolinite and dickite, the crystal order of both increases together with the proportion of dickite.

FTIR

The samples were analyzed using FTIR in transmission mode, as KBr pellets. Approximately 0.5 mg of kaolin was mixed with ~200 mg of KBr in a mortar and the pellets were prepared in a press. This preparation results in a random orientation of the particles that avoids effects related to preferred orientation. The analyses were carried out using a Perkin Elmer Spectrum One FTIR spectrometer (Beaconsfield, UK) with a CsI beamsplitter, in the range 4000–230 cm^{-1} , at 4 cm^{-1} resolution, by accumulation of eight spectra in each measurement.

The spectra were investigated in a systematic manner for features indicative of the relative proportions of kaolinite-dickite. Six such features were found (Figure 1). (1) The ratio between the intensity of the minima (*i.e.* intensity values between bands) in the OH-stretching region at 3675 and 3635 cm^{-1} (*i.e.* minimum at 3635 cm^{-1} / minimum at 3675 cm^{-1}); this ratio increases progressively with dickite proportion. (2) Position of the band at ~1115 cm^{-1} in the Si–O stretching complex; this band progresses from ~1115 to ~1118 cm^{-1} with increasing dickite proportion. (3) Difference between the frequency (in wavenumbers) of the bands at ~1030 and ~1000 cm^{-1} in the Si–O

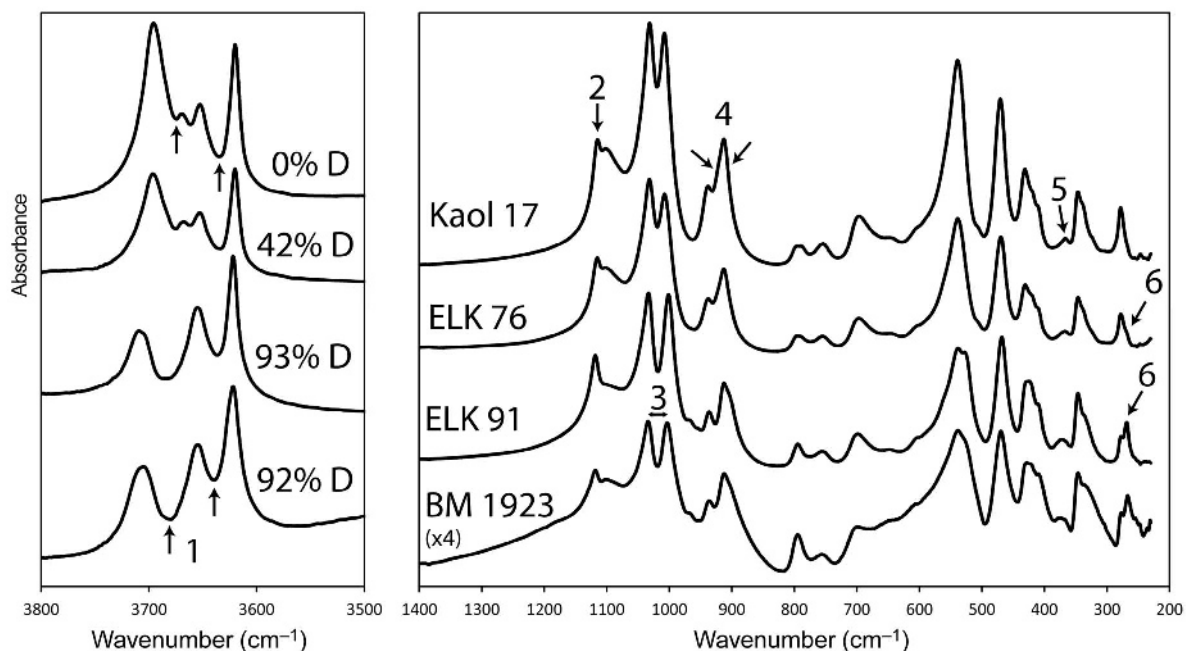


Figure 1. IR spectra of four selected samples covering the whole range of kaolinite–dickite relative abundance (indicated in the left panel). The intensity of the spectrum of BM 1923 has been increased ($\times 4$); some of the bands in this spectrum are wider. The spectral features used to quantify the relative proportions of the polytypes are indicated with arrows and numbered from 1 to 6, following the description in the text.

stretching complex; this difference increases with increasing dickite. (4) Intensity ratio of the bands generating shoulders at ~ 922 and ~ 900 cm^{-1} in the OH-bending region, on both sides of the main ~ 915 cm^{-1} band; the ratio of the 922 cm^{-1} band to the 900 cm^{-1} band decreases with increasing dickite (Frost 1998). (5) Position of the band at ~ 370 cm^{-1} , within the range of lattice vibrations, which moves from ~ 367 to ~ 372 cm^{-1} with increasing dickite. (6) Relative intensity of the band at ~ 268 cm^{-1} (only a shoulder in kaolinite), within the complex system in the range 300–250 cm^{-1} , corresponding to lattice vibrations; the intensity of this band increases with increasing dickite proportion.

The spectral features above were selected following investigation of the IR spectra in the present study. The following information about the assignment of the corresponding vibrations was collected from the literature. (1) The OH-stretching system has been studied by numerous authors and, while the main elements of the band assignment are understood, no complete agreement exists about the specific assignment of every individual band (Johnston *et al.*, 2008). The different shape of the OH-stretching spectral features in kaolinite and dickite is, however, known to emerge from the different configuration of hydrogen bonds due to the different distances between OH groups and O atoms across the interlayer that result from the different layer stacking and OH vector orientation (Johnston *et al.*, 2008). (2) The ~ 1118 cm^{-1} band has been assigned to the Si–O stretching vibration perpendicular to the layers (Farmer, 1974) and to Si–O symmetric stretching parallel to the layers (Balan *et al.* 2001); the frequency difference between kaolinite and dickite may arise from different Si–O distances. (3) The bands at ~ 1030 and 1000 cm^{-1} are assigned to in-plane Si–O–Si stretching (Farmer, 1974), and, more specifically, to antisymmetric stretching of equatorial Si–O bonds (Balan *et al.* 2001). (4) The band at ~ 922 cm^{-1} was assigned by Frost (1998) to libration (in-plane OH bending) of one of the three inner-surface OH groups in kaolinite. The band at ~ 900 cm^{-1} was assigned to libration of non-hydrogen-bonded inner OH groups both in kaolinite and dickite and this band is stronger in kaolinite (Frost, 1998). (5) No assignment was found for the ~ 370 cm^{-1} band. (6) The band at ~ 260 cm^{-1} was assigned tentatively by Frost (1997) to a vibration of the O–H–O group, involving hydroxyl groups hydrogen-bonded to oxide anions across the interlayer space.

The measurements of the relative band intensities above (numbers 4 and 6) were carried out by curve-fitting assuming Gaussian shapes, using the *GRAMS/AI* package from Thermo Galactic (Salem, New Hampshire, USA). Although Lorentzian shapes represent better the central part of IR bands, Gaussians were preferred because Lorentzian bands can have very long tails spanning unrealistically wide frequency ranges which distort the calculations. The region studied was first

deconvolved using the Fourier self-deconvolution function of the above package (sharpening of the bands that increases spectral resolution), which allowed us to establish very approximate band positions within the range. Then, part of the spectrum was selected in which the bands of interest were clearly bracketed between two minima, to perform the curve-fitting process within this specific range. The background in this area was calculated using a cubic or quartic equation and subtracted from the spectrum. Band positions were originally fixed at those values obtained from the deconvolution process, and band widths and heights were usually given a variation range. As the calculation converged, most or all variables were left entirely free, depending on the quality of the result, which was estimated from the homogeneity of band widths, comparison between results from different samples, and reproducibility of the results within samples. The areas of the bands of interest (Figure 2) were normalized to the total area of the fitted region.

The intensity of the spectra was measured as the height of the most intense band, at 1030 cm^{-1} , from a background line, established as a straight line linking spectral minima at ~ 1400 and 820 cm^{-1} . These intensities were corrected for the exact proportion of sample mixed with KBr.

RESULTS

The analysis of the IR spectral characteristics was compared with the proportion of kaolinite and dickite resulting from the XRD study (Figure 3). Great confidence is placed in the XRD results because they are based on the relative intensity of diffraction peaks diagnostic of kaolinite and dickite. The quantification process used several of these peaks at different θ angles and the results were averaged (Cuadros *et al.*, 2014). Comparison of the IR and XRD data from the present work and from others in the literature (Figure 3) shows that, in most cases, the data are grouped within a clear pattern, *i.e.* no clouds of data and very few outliers are present. One outlying value exists in one case (Figure 3e, open diamond at 0% dickite), where the frequency of the band indicated by Russell and Fraser (1994) for a kaolinite spectrum is above those detected in Keokuk and Kaol 17. Similarly, the frequency of the kaolinite band at ~ 1115 cm^{-1} given by Russell and Fraser (1994) is 1108 cm^{-1} (not shown in Figure 3f). Whether these differences are real or caused by a small error in the reading of the corresponding frequency (note that the ranges of values in the vertical axis in Figure 3e and 3f are small) is not known. The curve-fitting process of Kaol 17 for the bands near 915 cm^{-1} (Figures 2a, 3c) did not converge on a stable solution. The result shown here was obtained by fixing the band widths approximately proportional to their intensity. This result matched the calculation for Keokuk, which was stable,

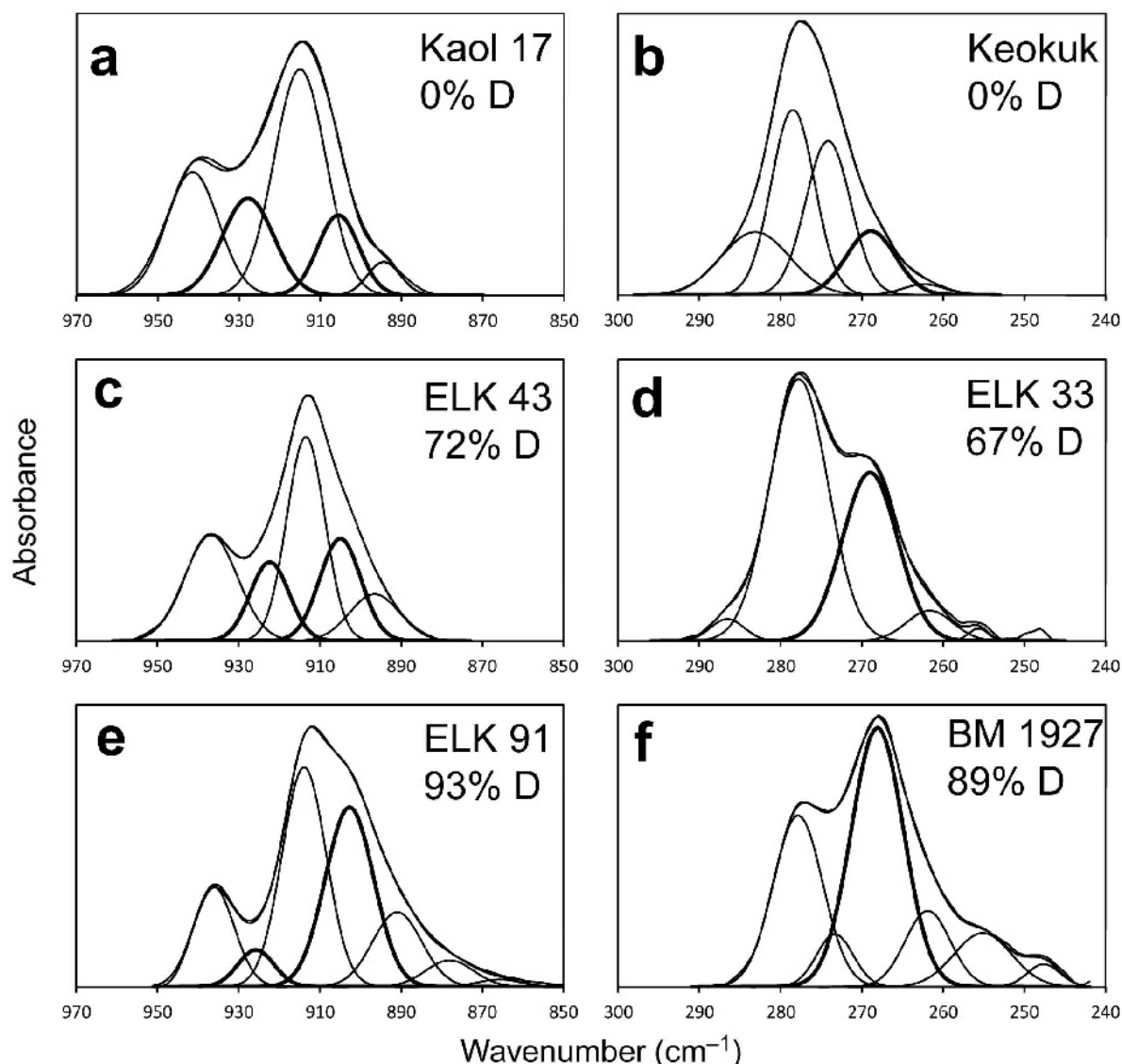


Figure 2. Decomposition of the spectra of selected samples to illustrate the changes taking place in the intensity of the bands used to quantify the relative proportions of kaolinite and dickite (D). The bands of interest are indicated with thicker lines (two bands each in parts a, c, e; one band each in parts b, d, f). The experimental and calculated spectra are almost coincident. The maxima of the bands of interest are at the following values (cm^{-1}): (a) 927, 905, (c) 922, 904, (e) 926, 902, (b) 267, (d) 268, (f) 268.

but the instability in the calculation for Kaol 17 indicates a large error in the result for this sample. The values taken from Fialips *et al.* (2003) and Russell and Fraser (1994) for dickite assume that the corresponding samples have no kaolinite component (Figure 3a,b,e,f).

Besides the departures from the main trends (Figure 3), the spectral values of KGa-2 did not correspond to those of Kaol 17 and Keokuk. For this reason KGa-2 was not included in the analysis. A very likely reason for the different behavior of KGa-2 is that it contains a significant amount of Fe ($1.15 \pm 0.02\%$ Fe_2O_3 ; Mermut and Cano, 2001), which can alter the frequency and relative intensities of IR bands. In fact, a low-intensity band at $\sim 880\text{ cm}^{-1}$ is present in the KGa-2

spectrum which corresponds to OH bending in AlOHFe groups.

DISCUSSION

Analysis of the present results shows a clear pattern in the change of the spectral characteristics studied. This pattern does not allow a sufficiently accurate quantification of the relative proportions of kaolinite and dickite in the whole range of concentrations, however. The pattern bends at the dickite-rich end of the series in four cases (Figure 3a–d) and the IR method loses resolution and therefore the ability to discriminate different proportions of the two polytypes in this range. In two other cases

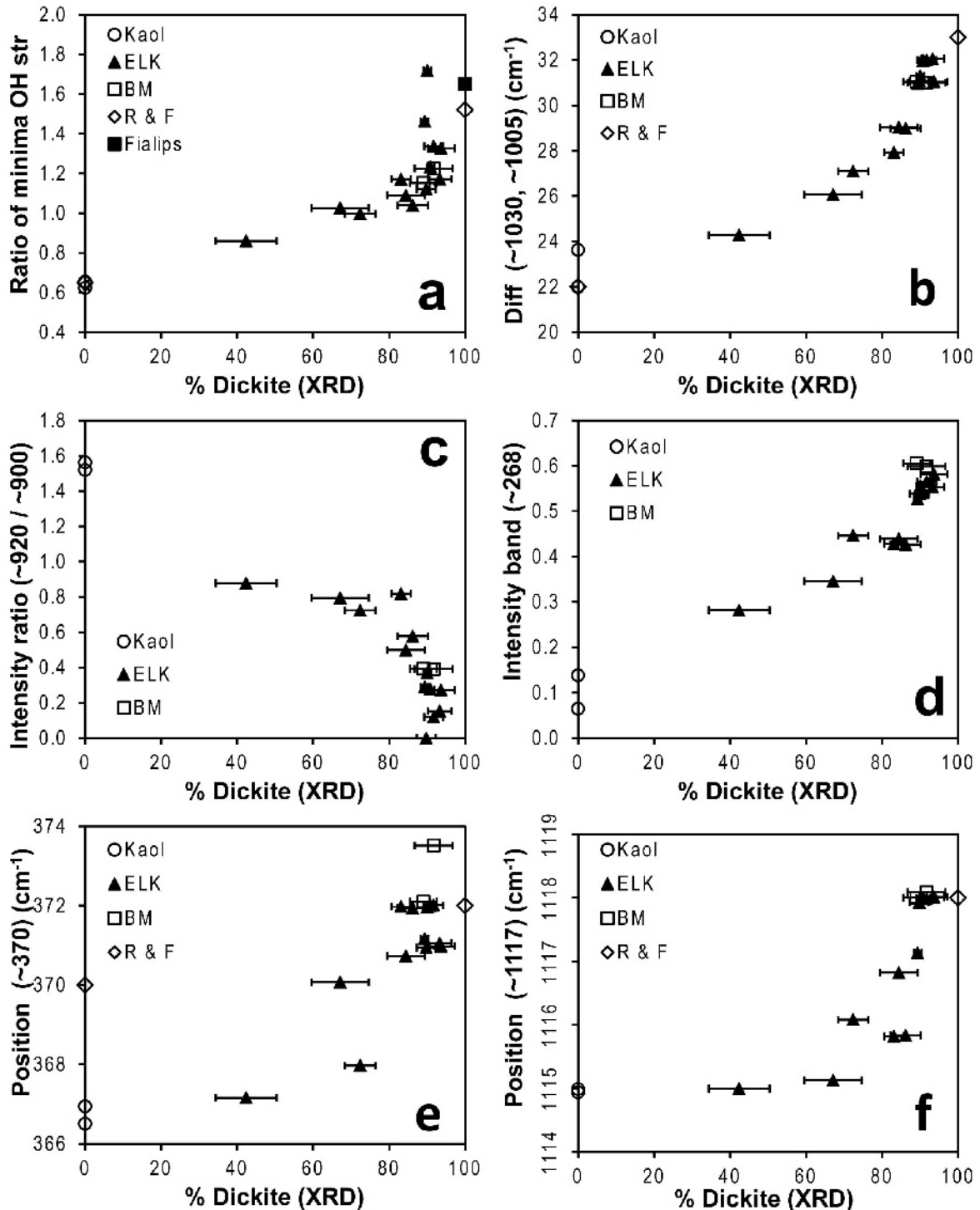


Figure 3. Plots of the proportion of dickite in the samples obtained from XRD (Cuadros *et al.*, 2014) and the IR spectral features (see text for a full explanation of these features). ELK corresponds to the ELK series, BM to the two dickites, and Kaol to the two kaolinites (see Methods). The numbers in parentheses in the vertical axis labels represent the centers of the bands investigated (cm^{-1}). Besides the data from the present study, data are also included from the literature for dickite (Fialips *et al.*, 2003) and for kaolinite and dickite (R and F: Russell and Fraser 1994). In these cases, the assumption is that the dickite did not contain any kaolinite. Error bars are 2σ standard deviation, and are smaller than the symbols used to represent the kaolinite samples. There are no error bars for the data from the literature

(Figure 3e,f), the lack of resolution of polytype concentrations occurs in the kaolinite-rich part of the series. The spectral test that displays the smallest bending and the greatest resolution in the entire kaolinite-dickite range is the measurement of the area of the band at $\sim 268\text{ cm}^{-1}$ (Figure 3d). Overall, the bending pattern (Figure 3), the existence of some outliers, and the uncertainty that the chemical composition introduces in the spectral characteristics of kaolinite and dickite indicate that IR spectroscopy does not quantify accurately the relative proportion of the two polytypes unless the crystal chemistry of the samples is sufficiently well understood and can be used to introduce corrections in the measured values that make them comparable and to display a linear trend.

The fact that analytical tests that use such different spectral characteristics all produced a curved pattern when compared with the XRD data (Figure 3) suggests that the reason for such a curved pattern is common to all of them. The existence of a mismatch between the development of the crystal structure (XRD features) and the atom bonding (IR features), as the reaction of kaolinite to dickite progresses, is unlikely. The reason is that interatomic distances and angles are related directly to the distances between atomic planes and their relative rotations and displacements. Another possibility is that XRD does not detect transformation toward the dickite end, while IR spectroscopy does. Such could be the case if the kaolinite domains at the last stages were so small that the corresponding XRD peaks were not visible, due to large width and low intensity. In this scenario, one would observe changes taking place in the IR features and little or no change in the XRD patterns, as occurs in Figure 3. This possibility encounters two difficulties, however. One is that the average coherent scattering domain size (CSDS) of kaolinite actually increases with burial (two processes take place, transformation of kaolinite into dickite and growth of kaolinite crystals; Cuadros *et al.*, 2014), which is exactly the opposite of what the explanation implies. The other difficulty is that the change in the approximate point in the vertical axis (IR features) from where departure from linearity occurs ($\sim 80\%$ dickite from XRD) in Figure 3a to 3d is 30–50% of the total change taking place in the entire transition. This would mean that XRD fails to detect as much as 30–50% of the transformation, which is very unlikely.

Brindley *et al.* (1986) noticed that the intensity of IR spectra of kaolinite of high crystal order and many of the dickites in their study was lower than that of the kaolinites with lower crystal order. This observation suggests that the intensity of mid-IR spectra is inversely correlated to crystal order, which was corroborated in this study. The normalized intensity of the spectra (intensity of the most intense band, at 1030 cm^{-1} ; see methods) was compared with the proportion of kaolinite and dickite from XRD (Figure 4a). The intensity of the IR spectrum generally decreases with increasing dickite

and this latter variable is likely to correlate positively with crystal order. The three kaolinite samples show very different IR spectral intensity, and their values correspond, from top to bottom, to KGa-2, Kaol 17 and Keokuk, in the correct sequence of increasing crystal order. Plotting the IR spectral intensity vs. a variable that reflects directly the crystal order shows the correlation existing between the two variables. The CSDS of several samples was used, measured from the width of the 001 peak (Cuadros *et al.*, 2014). The intensity of the IR spectra and the CSDS correlate negatively (Figure 4b). Such a correlation between the CSDS and the intensity of the IR spectra may follow a slightly different path for different groups of samples. However, the fact that this correlation exists, and that it is significant even when samples of very different origin and history are grouped together, is sufficient for the present discussion.

The decrease in intensity of the mid-IR spectrum with increasing crystal order is probably related to the phenomenon indicated by Johnston *et al.* (2008; and references therein) in relation to OH-stretching bands of kaolin minerals. When the size of the particle interacting with the IR radiation is similar to the IR wavelength the bands are distorted and widened (Johnston *et al.*, 2008). Brindley *et al.* (1986) found the spectral intensity decrease to affect the entire range of frequency in the mid-IR, as found also in the present study. The wavenumber range investigated in the present work, $230\text{--}4000\text{ cm}^{-1}$, corresponds to a wavelength range of $43.5\text{--}2.5\text{ }\mu\text{m}$. Poorly crystallized kaolins have particles with a size range below $2.5\text{ }\mu\text{m}$, as shown, for example, by Cuadros *et al.* (2014) who found that the average longest dimension in particles of Kaol 17, of intermediate particle size, is $2.5\text{ }\mu\text{m}$, with the other two average dimensions of 1.5 and $0.1\text{ }\mu\text{m}$. Low crystal-order kaolins have smaller particles than Kaol 17. In kaolins of high crystal order the number of large crystals increases and may reach large values. As the size of particles and the size of X-ray coherent scattering domains will typically grow together, the cause-effect link between intensity of the IR spectra and crystal order (apparent in Figure 4b) is reasonable.

The particle size and shape of the analyzed mineral can affect the IR spectrum in several ways, however. Only one of these influences the spectra in the present study, and it is discussed first. The other effects not influencing this study will be discussed briefly later. Fine particles are more efficient at absorbing IR radiation than coarse ones (Farmer, 1998). Such an effect is due to a number of interconnected reasons. The ideal situation for a transmission experiment is that in which the IR radiation is either absorbed by the mineral or is transmitted to the detector without any other significant interaction with the sample. Other phenomena take place, however, such as scattering, in which the radiation bounces from external or internal surfaces (imperfections, pores, etc.) of the analyzed particles.

Scatter of the IR radiation by the analyzed crystals is negligible for particle size well below the IR wavelength, but increases as particle size and wavelength become similar, which may reduce the proportion of absorbed radiation (van der Marel and Beutelspacher, 1976). Additionally, absorption is dependent on the surface area of the mineral analyzed. Samples consisting

of fine particles have larger surface areas than coarse ones and are more efficient absorbers (Dahm and Dahm, 2001). The phenomena above can account for the lower spectral intensity of the kaolins with higher crystal order in the present investigation.

Scattering can also cause changes in the spectral baseline due to IR radiation loss due to scattering rather than absorption (King *et al.*, 2004; Bassan, 2011). If severe, baseline modification can alter the apparent position of bands, especially if they are broad and/or have low intensity. The baselines in the spectra investigated here were all similar. The lower spectral intensity of the kaolins with high crystal order means that the ‘band intensity/baseline height’ ratio was smaller, but always large enough that there was no change to band positions or to any of the features investigated (Figures 1, 3). Further to the previous effects, the polarization of the crystals induced by IR radiation generates electric fields that: (1) interact with the macroscopic polarization field of the medium in which the sample is dispersed; and (2) affect bond vibrations in the sample depending on the relative orientation of the polarization and bond vibration (Farmer and Russell, 1966; Balan *et al.*, 2001). This interaction modifies IR spectra depending on structural symmetry and particle shape and size (Farmer, 1998; Balan *et al.*, 2001). Modifications of kaolin IR spectra due to kaolin particle size or crystal order have been recognized and associated with polarization effects (Farmer and Russell, 1964, 1966; Lombardi *et al.*, 1987; Farmer, 1998; Shoval *et al.*, 1999; Farmer, 2000; Balan *et al.*, 2001). The modifications recognized include: (1) OH-stretching band appears at 3686 or 3697 cm^{-1} in kaolinite and at 3643 or 3655 cm^{-1} in dickite; (2) Si–O stretching band is displaced in the range 1080–1107 cm^{-1} ; (3) band shifts in the range 689–697 cm^{-1} . None of these modifications corresponds to those investigated here (Figure 1). Some of the band displacements indicated above were observed when comparing the kaolinite samples KGa-2, API 17, and Keokuk, which cover a wide range of particle size, but the features investigated were the same for the kaolinites

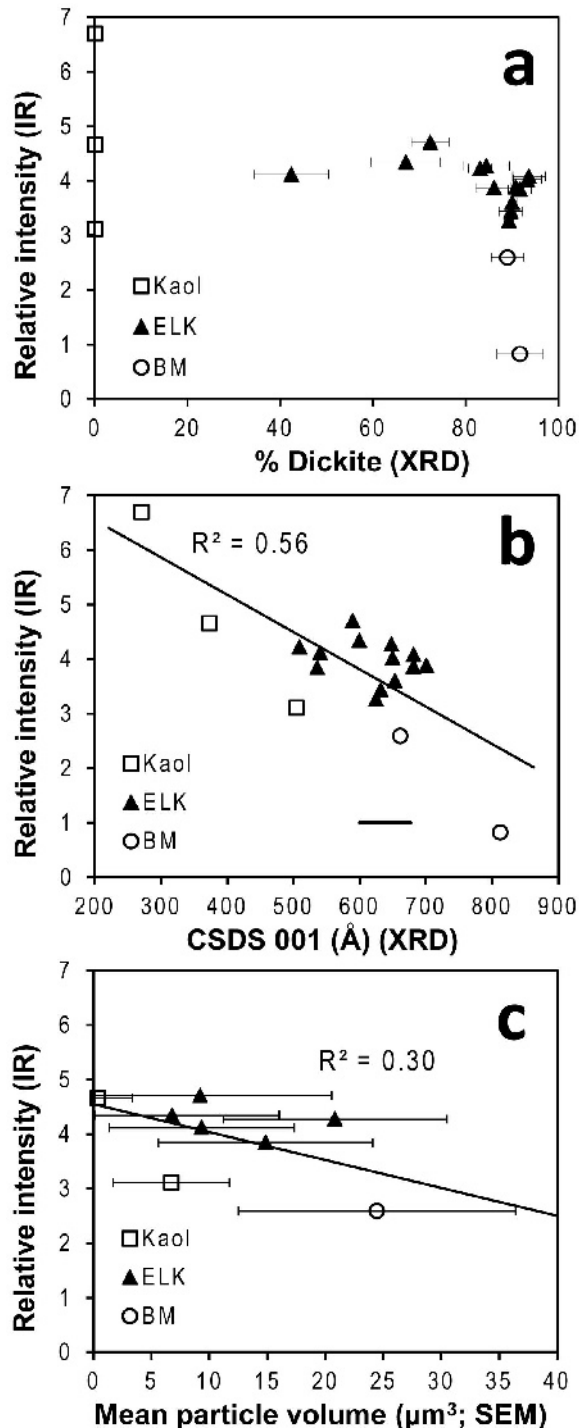


Figure 4. Relative intensity (see text for details) of the IR spectra of the studied samples vs. (a) dickite proportion from XRD (Cuadros *et al.*, 2014), (b) the coherent scattering domain size (CSDS, in Å) measured from the 001 XRD peak (Cuadros *et al.*, 2014), and (c) the mean particle volume as measured using SEM (Cuadros *et al.*, 2014). The correlations in (b) and (c) include all data points and indicate a significant negative correlation between spectral intensity and CSDS, and a low-significance correlation with mean particle volume. Error bars in (a) and (c) are 2σ standard deviation. There are no individual error values for (b), where the horizontal bar is the 1σ standard deviation from the calculation of the average CSDS from the 001 peak of samples with $>80\%$ dickite in Cuadros *et al.* (2014). This bar is provided as an approximation to the errors involved.

(Figure 3). The investigated features were chosen because they changed systematically with kaolinite-dickite composition, and thus they must depend mainly on the kaolin polytype.

The variable that affects IR spectral intensity is the size of the particles, rather than the size of the coherently X-ray diffracting crystal domains within them, although both are correlated, as stated above. The particles are made up of crystals or coherent domains of size that will typically grow with that of the particles. Accordingly, the relationship between the actual particle size and the intensity of the IR spectra was investigated, using particle-size data from Cuadros *et al.* (2014). The average particle volume was used, as the product of the three average particle dimensions, in order to involve all three dimensions in the analysis. The IR spectrum intensity and the mean particle volume of a group of kaolinite and kaolinite-dickite (K-D) samples display a negative correlation of low significance (Figure 4c). However, the low R^2 value of 0.3 does not disprove the link between the two variables for several reasons. One is the reduced number of samples for which particle size is available (eight data points in Figure 4c; 18 data points in Figure 4b); in particular, the kaolins with the lowest and highest crystal order are missing, samples which would be helpful in better defining the correlation. Another reason is that the relation between average particle dimensions and the distribution of particle size is complex (large standard deviation in Figure 4c) and variable between samples (see figure 8 in Cuadros *et al.*, 2014). Finally, the extent to which the average particle volume represents the decreased IR absorption is not the same across samples because absorption depends on the entire particle-size distribution, which is probably different from sample to sample. The low correlation between IR spectral intensity and particle mean volume (Figure 4c) is probably due to the above limitations, and a link between particle size and the intensity of the IR spectra in the kaolins does exist, as observed by other authors (Brindley *et al.*, 1986; Johnston *et al.*, 2008).

The increase in particle size is a potential explanation for the curved patterns recorded here (Figure 3), if the growth of kaolinite-dominated particles does not progress as much as that of dickite-dominated particles, so that in the latter stages of the kaolinite-dickite series the intensity of the IR radiation absorbed from kaolinite-rich particles is greater than that from dickite-rich particles. The X-ray coherent scattering domains of kaolinite and dickite were found (Cuadros *et al.*, 2014) to be similar at >80% dickite, *i.e.* the kaolinite crystal domains grow as large as the dickite domains. However, the coherent scattering domains are different from and smaller than the particles. Previous evidence from other kaolinite-dickite samples (Kogure and Inoue, 2005a; Johnston *et al.*, 2008) has shown that particles can contain both kaolinite and dickite domains. This is a natural

possibility following the interpretation from Cuadros *et al.* (2014) that the reaction of these samples was mainly solid state, although another TEM study of one sample from the Frøy oil field identified only single polytypes within grains (Kogure and Inoue, 2005b). A model was created in order to test the effect of differential particle growth in kaolinite- and dickite-dominated samples. For the sake of simplicity, the model considers that kaolinite and dickite particles are independent (each particle contains only one of the two polytypes). The model calculates the progressive growth of the particle volume and relates it through a simple, arbitrary formula to a corresponding IR spectral intensity of the particle population of kaolinite and dickite. The starting point corresponds to a kaolinite sample with particle dimensions taken from the average dimensions measured for Kaol 17 (Cuadros *et al.*, 2014), with a particle volume of $0.38 \mu\text{m}^3$. The final point for kaolinite particles, at the end of the series, corresponds to the average particle volume of Keokuk kaolinite, $6.75 \mu\text{m}^3$ (Cuadros *et al.*, 2014). For dickite, the final point is $14 \mu\text{m}^3$, as the average particle growth measured by Cuadros *et al.* (2014; taken from the correlation lines in their figure 8). The model uses three scenarios. In the first, the maximum particle size for kaolinite and dickite is reached at 80% dickite content in the sequence (Figure 5, top). In the second scenario, the maximum particle growth, also for both polytypes, is reached at 90% dickite (Figure 5, middle panel). In the third scenario, the particle growth is maintained throughout the entire sequence; *i.e.* the maximum particle size for both polytypes is reached at 100% dickite (Figure 5, bottom). In every case, kaolinite and dickite particles grow at constant steps in the sequence, although the steps are different for each polytype because their final particle size is different.

The intensity of the IR spectrum was calculated as a function of the particle volume, using the formula

$$I = 1 - mV \quad (1)$$

where I is the spectrum intensity, m is a variable parameter (slope), and V is the particle volume. The main parameters from the three scenarios (Table 2) are discussed below. The results are shown as plots (Figure 5) representing the IR spectral intensity from kaolinite (line K) and dickite (line D) particles, both of them normalized to the intensity from the original K particles (*i.e.* % dickite = 0), and the relative contribution of both to the spectral intensity (line D–K). The D–K line is the model of the patterns observed in Figure 3. The dashed line is the diagonal in the plot, included to observe better the departure of line D–K from linearity. The specific values of lines K and D are not directly comparable between plots because they are normalized to different original spectral intensities (the original intensity, at % dickite = 0, varies with the value of the slope m , which is different for each model

scenario), but the lines D–K are comparable between plots. The slopes (m) that were selected to be displayed (Figure 5) correspond to those that create a maximum curvature of D–K lines. The results are similar to and compatible with the patterns in Figure 3. First, the data show an almost linear interval in the progression of the kaolinite-dickite spectral features with respect to the dickite content, followed by a curved interval from

80–90% dickite content (Table 2). The % change of the IR features (vertical axis in Figure 5) in the linear interval in the D–K line ranges 57–68% of the total observed change, in agreement with those observed of 50–68% (Figure 3). One element of the model is the total reduction of spectral intensity generated by the increase in particle size. Experimentally, the relative decrease of spectral intensity from Kaol 17 (modeled here) to a K-D sample with 92% dickite is from 4.66 to 0.82 (relative units), with a ratio between the two of 5.6. The model generates ratios between 20 and 4.8 (Table 2). According to the results (Table 2), the most realistic model scenario would be one in which particle growth stops when the overall dickite composition is ~80%.

This model demonstrates that the pronounced departure from linearity in Figure 3 can be explained by effects related to differential absorption of the IR radiation by kaolin particles with different sizes. The IR features investigated (Figure 3) are very different, some relating to band position and some to band intensity ratios. Obviously, the relative IR band intensities of kaolinite and dickite depend on the relative intensity of the corresponding spectra that contribute to the composite spectrum. This is also true for band positions because the maxima of the bands that were analyzed are displaced between the kaolinite and dickite values in proportion to the intensity of the corresponding spectrum. The evolution of the several individual features is not expected to be identical, as observed (Figure 3), but the curved pattern generated by differential IR absorption should be present in all cases, as is the case here (Figure 3). In a burial kaolinite-dickite sequence, kaolin particles grow with increasing dickite content, even if not in a regular or constant way (Lanson *et al.*, 2002; Cuadros *et al.*, 2014). According to the present interpretation, kaolinite particles must grow to a smaller maximum size than dickite particles, otherwise the IR-particle interaction would be the same with particles of both polytypes and any comparison between IR and XRD features would be linear. This is because absorption is a function of the overall surface area of the absorbing particles (Dahm and Dahm, 2001). Experiments in the near-infrared with

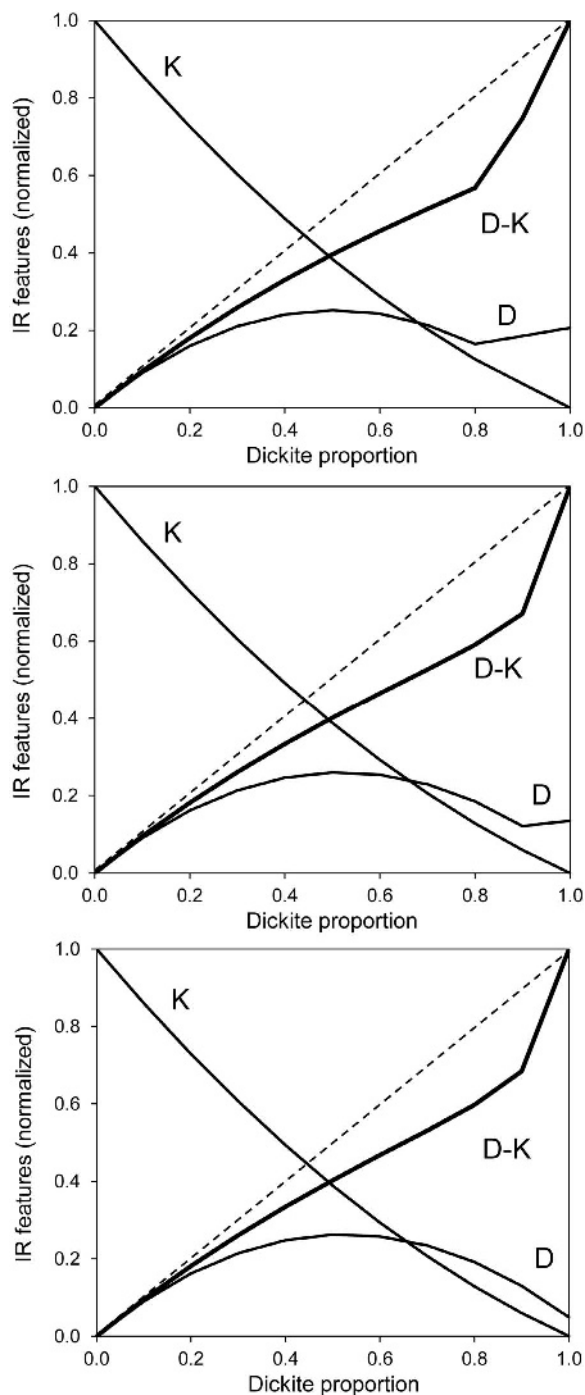


Figure 5. Model of the evolution of the IR spectral features in a series of progressive reactions of kaolinite to dickite, where the intrinsic intensity of IR spectra of both kaolinite and dickite decreases as the reaction progresses (due to increasing particle size). From top to bottom, the maximum particle size of the kaolins is reached at 80, 90, and 100% dickite content, respectively. The K and D lines indicate the change in intensity of the IR spectrum corresponding to kaolinite and dickite, normalized to the intensity of the original kaolinite spectrum. The D–K line shows the evolution of the relative intensity of the dickite features during the transformation (contribution of the dickite IR spectrum to the spectrum of the kaolinite-dickite mixture). The diagonal dashed line is a visual aid to observe the departure of the D–K line from linearity.

Table 2. Parameters from the models in Figure 5. % Dickite value at which growth of the particles stops; slope in the model equations; % dickite and % change of the IR features (vertical axis) at which the modeled line has its sharpest bending point; and the spectral intensity 'original kaolinite/final dickite' ratio.

Model	% Dickite at which growth ends	Slope in equation (<i>m</i>)	% Dickite at sharpest bending point	% IR change at sharpest bending point	Intensity ratio
1	80	0.057	80	57	4.8
2	90	0.062	90	67	7.4
3	100	0.068	90	68	20

mixtures of seeds of different nature have shown: (1) a linear correlation between IR absorbance and the known proportion of each type of seed if their size is the same; but (2) a non-linear correlation if the seeds have different size. In the real kaolinite–dickite sequence, particles may contain dickite and kaolinite crystals or domains within crystals. However, in all likelihood the growth of these crystals or domains observed experimentally (Cuadros *et al.*, 2014) means that they tend to exclude each other, so that particles would become dominated by one of the two polytypes. What could be the reason for kaolinite-dominated particles to stop growth at a smaller maximum size than dickite-dominated particles even if they are in the same environment? The answer could be in the standard Gibbs free energy difference between them (0.07–25 kJ/mol: Anovitz *et al.*, 1991; De Ligny and Navrotsky 1999; Fialips *et al.*, 2001, 2003; Sato *et al.*, 2004), even if it is small. Alternatively, the reason could be in the way particles grow. Signs of particle coalescence were found in the particles studied here, using SEM, by Cuadros *et al.* (2014). If coalescence is an important mechanism of particle growth, then as the dickite proportion increases, the chance that kaolinite particles meet and coalesce decreases. At the same time, kaolinite particles probably cannot coalesce with dickite particles frequently due to the different crystal structure. According to the model, at ~80% dickite composition all particles would stop growing. This result is dependent on the chosen linear relation between particle volume and spectrum intensity, and may not be correct. It is, however, possible that particles stop growing at some stage because bigger particles, on average, are not stable, whereas the proportion of dickite layers and the X-ray coherent scattering domains of kaolinite and dickite may still grow within particles.

If the interpretation proposed here is correct, the use of IR spectroscopy for the quantification of kaolinite and dickite in a reaction series is problematic in the dickite-rich section, where the spectral features change abruptly in a very short range of kaolinite-dickite composition. This effect is intrinsic to the study and cannot be avoided or corrected in a trivial way. It is related to the fact that the kaolin particle size increases differentially with increasing dickite. Prolonged grinding of the samples until particle size is below the IR wavelength may be an option, although this may jeopardize the quantification

by causing extensive dislodging between layers. Any differential dislodging of layers between the polytypes would alter the original polytype proportion. Perhaps the best option is to choose the spectral feature that changes in the most linear fashion as compared to XRD results (*e.g.* Figure 3d).

ACKNOWLEDGMENTS

C. Fialips, D. Beaufort, and S. Hillier are thanked for kindly providing the North Sea kaolinite-dickite series samples and the Keokuk kaolinite. C. Fialips is also thanked for discussion from the early inception of the study to the stage of data interpretation. R.V. and A.T. were funded by the Erasmus program of the EU via the University of Huelva, Spain. The discussion with and comments by two anonymous reviewers, the Associate Editor, and the Editor-in-Chief helped to improve this manuscript and the authors are grateful to them.

REFERENCES

- Anovitz, L.M., Perkins, D., and Essene, E.J. (1991) Metastability in near-surface rocks in the system $\text{Al}_2\text{O}_3\text{-SiO}_2\text{-H}_2\text{O}$. *Clays and Clay Minerals*, **39**, 225–233.
- Balan, E., Saitta, A., Mauri, F., and Calas, G. (2001) First-principles modeling of the infrared spectrum of kaolinite. *American Mineralogist*, **86**, 1321–1330.
- Balan, E., Refson, K., Blanchard, M., Delattre, S., Lazzeri, M., Ingrin, J., Mauri, F., Wright, K., and Winkler, B. (2008) Theoretical infrared absorption coefficient of OH groups in minerals. *American Mineralogist*, **93**, 950–953.
- Balan, E., Delattre, S., Guillaume, M., and Salje, E. (2010) Low-temperature infrared spectroscopic study of OH-stretching modes in kaolinite and dickite. *American Mineralogist*, **95**, 1257–1266.
- Bassan, P. (2011) Light scattering during infrared spectroscopic measurements of biomedical samples. PhD thesis, University of Manchester, UK, 120 pp.
- Beaufort, D., Cassagnabère, A., Petit, S., Lanson, B., Berger, G., Lacharpagne, J.C., and Johansen, H. (1998) Kaolinite to dickite reaction in sandstone reservoirs. *Clay Minerals*, **33**, 297–316.
- Benco, L., Tunega, D., Hafner, J., and Lischka, H. (2001) Orientation of OH groups in kaolinite and dickite: Ab initio molecular dynamics study. *American Mineralogist*, **86**, 1057–1065.
- Brindley, G.W., Kao, C.-C., Harrison, J.L., Lipsicas, M., and Raythatha, R. (1986) Relation between structural disorder and other characteristics of kaolinites and dickites. *Clays and Clay Minerals*, **34**, 239–249.
- Cassagnabère, A. (1998) Caractérisation et interprétation de la transition kaolinite-dickite dans les réservoirs à hydrocarbures de Froy et Rind (Mer du Nord), Norvège. PhD thesis,

- Université de Poitiers, France, 214 pp.
- Cuadros, J., Vega, R., Toscano, A., and Arroyo, X. (2014) Kaolinite transformation into dickite during burial diagenesis. *American Mineralogist*, **99**, 681–695.
- Dahm, D.J. and Dahm, K.D. (2001) The physics of near-infrared scattering. Pp. 1–17 in: *Near-Infrared Technology in the Agricultural and Food Industries* (P.W. Williams and K. Norris, editors). American Association of Cereal Chemists, St. Paul Minnesota, USA.
- De Ligny, D. and Navrotsky, A. (1999) Energetics of kaolin polymorphs. *American Mineralogist*, **84**, 506–516.
- Farmer, V.C. (1974) The layer silicates. Pp. 331–364 in: *The Infrared Spectra of Minerals* (V.C. Farmer, editor). Monograph 4, Mineralogical Society, London.
- Farmer, V.C. (1998) Differing effects of particle size and shape in the infrared and Raman spectra of kaolinite. *Clay Minerals*, **33**, 601–604.
- Farmer, V.C. (2000) Transverse and longitudinal crystal modes associated with OH stretching vibrations in single crystals of kaolinite and dickite. *Spectrochimica Acta Part A*, **56**, 927–930.
- Farmer, V.C. and Russell, J.D. (1964) The infrared spectra of layer silicates. *Spectrochimica Acta*, **20**, 1149–1173.
- Farmer, V.C. and Russell, J.D. (1966) Effects of particle size and structure on the vibrational frequencies of layer silicates. *Spectrochimica Acta*, **22**, 389–398.
- Fialips, C.I., Navrotsky, A., and Petit, S. (2001) Crystal properties and energetics of synthetic kaolinite. *American Mineralogist*, **86**, 304–311.
- Fialips, C.-I., Majzlan, J., Beaufort, D., and Navrotsky, A. (2003) New thermochemical evidence on the stability of dickite vs. kaolinite. *American Mineralogist*, **88**, 837–845.
- Frost, R. (1997) The structure of the kaolinite minerals – a FT-Raman study. *Clay Minerals*, **32**, 65–77.
- Frost, R.L. (1998) Hydroxyl deformation in kaolins. *Clays and Clay Minerals*, **46**, 280–289.
- Hayes, J.B. (1936) Kaolinite from Warsaw geodes, Keokuk Region, Iowa. *Iowa Academy of Sciences Proceedings*, **70**, 261–272.
- Johnston, C., Kogel, J., Bish, D., Kogure, T., and Murray, H. (2008) Low-temperature FTIR study of kaolin-group minerals. *Clays and Clay Minerals*, **56**, 470–485.
- Kerr, P.F. and Kulp, J.L. (1949) Reference clay localities – United States. In: *American Petroleum Institute, Project 49, Clay Mineral Standards, Preliminary Report no. 2*, 24–25. Columbia University, New York.
- King, P.L., Ramsey, M.S., McMillan, P.F., and Swayze, G. (2004) Laboratory Fourier transform infrared spectroscopy methods for geological samples. Pp. 57–92 in: *Infrared Spectroscopy in Geochemistry, Exploration Geochemistry and Remote Sensing* (P.L. King, M.S. Ramsey, and G.A. Swayze, editors). Mineralogical Association of Canada.
- Kogure, T. and Inoue, A. (2005a) Stacking defects and long-period polytypes in kaolin minerals from a hydrothermal deposit. *European Journal of Mineralogy*, **17**, 465–473.
- Kogure, T. and Inoue, A. (2005b) Determination of defect structures in kaolin minerals by high-resolution transmission electron microscopy (HRTEM). *American Mineralogist*, **90**, 85–89.
- Lanson, B., Beaufort, D., Berger, G., Bauer, A., Cassagnabère, A., and Meunier, A. (2002) Authigenic kaolin and illitic minerals during burial diagenesis of sandstones: a review. *Clay Minerals*, **37**, 1–22.
- Lindberg, J.D. and Smith, M.S. (1974) Visible and near infrared absorption coefficients of kaolinite and related clays. *American Mineralogist*, **59**, 274–279.
- Lombardi, G., Russell, J.D., and Keller, W.D. (1987) Composition and structural variations in the size fractions of a sedimentary and a hydrothermal kaolin. *Clays and Clay Minerals*, **35**, 321–335.
- Mermut, A.R. and Cano, A.F. (2001) Baseline studies of the Clay Minerals Society Source Clays: chemical analyses of major elements. *Clays and Clay Minerals*, **49**, 381–386.
- Moll, W., Jr (2001) Baseline studies of the Clay Minerals Society Source Clays: Geological origin. *Clays and Clay Minerals*, **49**, 374–380.
- Prost, R., Dameme, A., Huard, E., Driard, J., and Leydecker, J.P. (1989) Infrared study of structural OH in kaolinite, dickite, nacrite, and poorly crystalline kaolinite at 5 to 600 K. *Clays and Clay Minerals*, **37**, 464–468.
- Robin, V., Petit, S., Beaufort, D., and Prêt, D. (2013) Mapping kaolinite and dickite in sandstone thin sections using infrared microspectroscopy. *Clays and Clay Minerals*, **61**, 141–151.
- Russell, J.D. and Fraser, A.R. (1994) Infrared methods. Pp. 11–67 in: *Clay Mineralogy: Spectroscopic and Chemical Determinative Methods* (M.J. Wilson, editor). Chapman & Hall, London.
- Sato, H., Ono, K., Johnston, C., and Yamagishi, A. (2004) First-principle study of polytype structures of 1:1 dioctahedral phyllosilicates. *American Mineralogist*, **89**, 1581–1585.
- Shoval, S., Yariv, S., Michaelian, K., Boudeulle, M., and Panczer, G. (1999) Hydroxyl-stretching bands ‘A’ and ‘Z’ in Raman and infrared spectra of kaolinites. *Clay Minerals*, **34**, 551–563.
- Shoval, S., Yariv, S., Michaelian, K., Boudeulle, M., and Panczer, G. (2002) Hydroxyl-stretching bands in polarized micro-Raman spectra of oriented single-crystal Keokuk kaolinite. *Clays and Clay Minerals*, **50**, 56–62.
- van der Marel, H.V. and Beutelspacher, H. (1976) *Atlas of Infrared Spectroscopy of Clay Minerals and their Admixtures*. Elsevier, Amsterdam.
- Zimmerle, W. and Rösch, H. (1990) Petrogenetic significance of dickite in European sedimentary rocks. *Zentralblatt für Geologie und Paläontologie Teil I*, 1175–1196.

(Received 21 January 2014; revised 3 April 2015; Ms. 841; AE: S. Petit)